Effect of thermal pretreatment and nanosilica addition on limestone performance at Calcium-Looping conditions for Thermochemical Energy Storage of Concentrated Solar Power

Jose Manuel Valverde*[a], Manuel Barea-López[b], Antonio Perejón[b,c], Pedro E. Sánchez-Jiménez[b], Luis A. Pérez-Maqueda[b]

[a]Faculty of Physics, University of Seville, Avenida Reina Mercedes s/n, 41012 Sevilla, Spain.

[b]Instituto de Ciencia de Materiales de Sevilla (C.S.I.C.-Universidad de Sevilla). C. Américo Vespucio 49, Sevilla 41092. Spain.

[c]Departamento de Química Inorgánica, Facultad de Química, Universidad de Sevilla, Sevilla 41071, Spain.

*Corresponding author: jmillan@us.es

Abstract

The share of renewable energies is rapidly growing partly in response to the urgent need of mitigating CO_2 emissions from fossil fuel power plants. However, cheap and efficient large-scale energy storage technologies are not yet available to allow for a significant penetration of renewable energies into the grid. Recently, it has been proposed a potentially low-cost and efficient thermochemical energy storage (TCES) system based on the integration of the Calcium Looping (CaL) process into Concentrated Solar Plants (CSP). The CaL process relies on the multicycle carbonation/calcination of CaO, which can be derived from calcination of widely available, cheap and non-toxic natural limestone ($CaCO_3$). This work explores the effect on the multicycle activity of limestone derived CaO of thermal pretreatment under diverse atmospheres and the addition of nanosilica, which would expectedly hinder CaO grain sintering. Importantly, optimum CaL conditions for CSP energy storage differ radically from those used in the application of the CaL process for CO_2 capture. Thus,

calcination should be ideally carried out under low CO_2 partial pressure at moderate temperature (below 750ºC) whereas CO_2 concentration and temperature should be high for carbonation in order to maximize thermoelectric efficiency. When subjected to carbonation/calcination cycles at these conditions, limestone performance is critically dependent on the type of pretreatment. Our results indicate that the multicycle CaO activity is correlated with the size of the particles and the CaO pore size distribution. Thus, CaO activity is impaired as particle size is increased and/or CaO pore size is decreased. These observations suggest that pore plugging poses a main limitation to the multicycle performance of limestone derived CaO at the optimum CaL conditions for TCES in CSP, which is supported by SEM analysis. Strategies to enhance the performance of natural limestone at these conditions should be therefore oriented towards minimizing pore plugging rather than CaO grain sintering, which stands as the main limitation at CaL conditions for CO_2 capture.

1. Introduction

The deployment of renewable energies, mainly solar and wind, has risen exponentially in the last years. In the 21th Conference of Parties (COP21), countries agreed to limit the increase in the global surface temperature below 2.0 ºC in 2100.[1] For achieving such ambitious goal, power production from renewable energy sources must be massively incorporated into the grid in the short to medium term. To this end, it is mandatory to develop large-scale energy storage technologies that allow overcoming the inherently intermittent nature of the principal renewable energy sources (solar and wind). Due to the huge-scale of the problem and to be competitive against fossil fuels, these new energy storage technologies must be efficient, affordable and environmental friendly.

Concentrated solar thermal power (CSP) is considered as a promising renewable energy technology to replace fossil fuel plants for grid power production as it offers the possibility of large scale electricity generation with potentially cheap thermal energy storage.[2-4] Conventional coal fired power plants (CFPP) burn coal to generate a high temperature and high pressure water steam, which expands into a turbine to produce mechanical work according to a Rankine cycle. The main difference between conventional CFPP and CSP is that, in the latter, the boiler is replaced by a heliostats

distributed system and a central tower in the case of CSP with tower technology that concerns us in the present paper. Heliostats concentrate solar irradiation in a central receiver at the top of the tower where heat is transferred to a fluid for generating electricity. Currently, a number of CSP demonstration plants are under operation worldwide incorporating thermal energy storage to generate electricity in the absence of direct solar irradiation. When available, direct solar irradiation is used to heat a so-called HTF (heat transfer fluid) consisting of a mixture of molten salts with high heat capacity. The solar salt is carried to a hot salts tank where energy is stored in the form of sensible heat with an energy density near 0,8 GJ/m^3.[5] On demand, the hot salt is circulated to a steam generator system where heat is transferred to water vapour while the cold salt is stored in a cold salts tank. However, the use of molten salts poses serious inconveniences that hinder the competitiveness of CSP with this type of energy storage. One of them is a limitation of the salt upper temperature due to its decomposition near 600ºC, which does not allow to achieve sufficiently high thermo-electric efficiencies as compared with fossil fuels. Another relevant issue is the high solidification point of the molten salts (between 120ºC and 220ºC), which makes it necessary to keep the salts at temperatures above these values leading to important heat losses especially during the night hours in desert zones at high altitude where CSP technology allocation is more appropriate. In addition, molten salts are very corrosive, which requires the installation of costly materials for pipes and valves. Solar salts commonly considered for thermal energy storage (TES) are the binary KNO_3-Na/NO_3 system, the ternary systems $NaNO_2$-$NaNO_3$-KNO_3 and the two ternary additive systems $Ca(NO_3)_2$-$NaNO_3$-KNO_3 and $LiNO_3$-KNO_3-$NaNO_3$. A comprehensive and concise review on TES systems based on molten salts including their thermophysical properties and novel salt formulations may be found in refs [6-9].

An alternative energy storage system to thermal energy storage in the form of sensible heat is Thermochemical Energy Storage (TCES), currently under R&D.[10-11] Essentially, TCES consists of using the potentially high temperatures attainable in the solar receiver to carry out an endothermic chemical reaction. The reaction by-products are stored individually and, when energy is needed, they are brought together to drive the exothermic reverse reaction. Some important advantages of TCES versus sensible heat storage in molten salts are the possibility of storing energy permanently with a

relatively high density and the potentially high efficiencies attainable by properly selecting the reacting systems at the relevant operation temperatures.[12]

Searching for a reversible reaction that better suits the characteristics of CSP plants with tower technology is a key issue. The materials to be used should allow affordable operation costs and the turning point of the reversible reaction must fit into the range of operating temperatures.[13] In this context, the Calcium Looping (CaL) process satisfies the requirements for a feasible TCES integration in CSP with tower technology.[14] The CaL process is based on the carbonation/calcination reaction of CaO (eq.1).

$$CaO_{(s)} + CO_{2(g)} \rightleftarrows CaCO_{3(s)} \quad ; \Delta H_r^0 = -178 \text{ kJ/mol} \qquad (1).$$

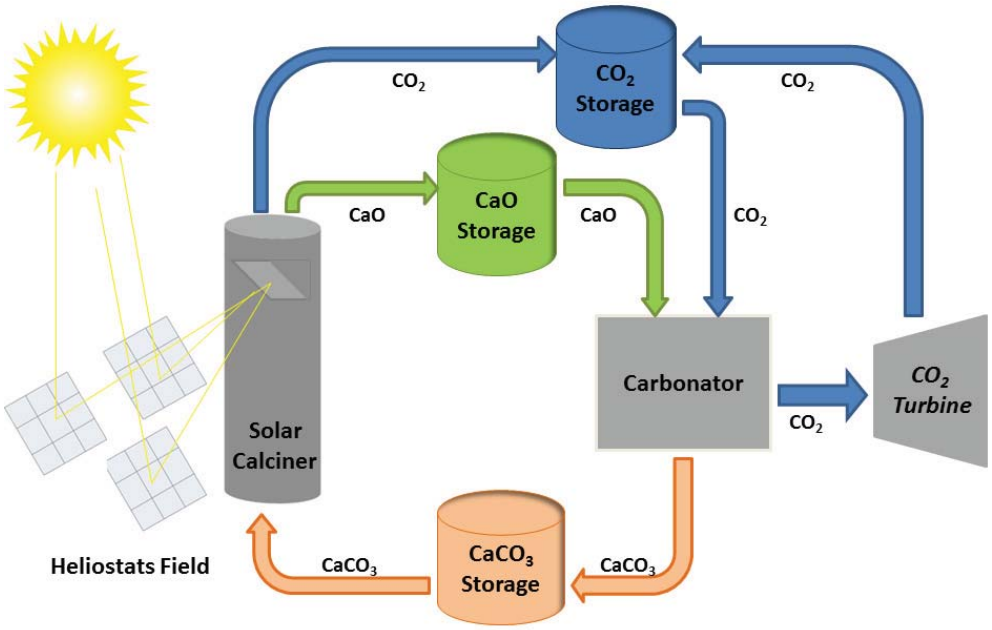

Fig. 1. Flow diagram of the CSP-CaL integration for Thermochemical Energy Storage

The use of the CaL process for TCES in CSP has many potential advantages such as the wide availability of limestone (almost 100% $CaCO_3$), its low cost, non-toxicity, and the high energy density attainable from the reaction enthalpy (~3.2 GJ/m^3).[13] A recently proposed scheme for the CaL- CSP integration leads to a potentially high thermoelectric efficiency using a closed CO_2 cycle for the carbonation reaction to generate electric power through a Brayton cycle as shown in the flow diagram of Fig. 1.[15] In this integration scheme, concentrated solar energy is used to carry out the calcination reaction. The CO_2 and CaO streams stemming from calcination are passed through a heat exchanger network to extract their sensible heat after which they are stored at ambient temperature. CaO solids are circulated into a solids reservoir whereas the CO_2 gas stream is stored in reasonably sized tanks under high pressure (~75 bar) at supercritical conditions by means of intercooling compression. Thus, besides of sensible and thermochemical energy storage, this integration includes energy storage also in the form of compressed gas (with a round trip efficiency of about 67% by using a compression-expansion train). On the other hand, a main advantage of the CSP-CaL integration is that the reactants can be stored at ambient temperature as opposed to molten salts, which must be kept always at temperatures over ~200°C to avoid solidification. Thermochemical stored energy is released in the carbonator on demand through the exothermic carbonation reaction. Thus, the CO_2 exiting the carbonator at high temperature over the stoichiometric ratio is used as heat gas carrier to generate electric power by means of a gas turbine in a closed circuit. Carbonation may be carried out at high temperature (>850ºC) under high CO_2 partial pressure to maximize the thermoelectric efficiency, which allows overcoming current temperature limits (T~550-600°C) in commercial CSP plants wherein heat is stored in molten salts. Thus, predicted efficiencies for this integration (above ~45%) are significantly higher than the efficiency achieved by using sensible heat storage in molten salts. The interested reader is referred to ref. [15], where a detailed energy integration study based on pinch-analysis methodology has been presented.

The multicycle CaO conversion (ratio of mass of CaO carbonated to initial mass in each cycle) in short residence times plays a relevant role on the CSP-CaL integration as any significant decay of it with the number of cycles would hinder the global plant efficiency.[15-16] A further important issue to consider for storing the maximum amount of energy during solar hours is that the calcination reaction should be completely achieved

as fast as possible and at the lowest possible temperature. From a techno-economical point of view, lowering the calcination temperature and shortening the reaction time would allow the use of relatively cheap volumetric receivers based of low cost metal alloys capable of working at temperatures up to 800ºC.[17] Thus, it has been shown that the use of high thermal conductivity gases such as helium or super-heated steam would enhance calcination at reduced temperatures (below 750ºC).[18] These gases could be separated from the CO_2 released in the calcination reaction to store it in compression tanks as pure as possible whereas He or super-heated steam is recirculated to be reused in the calcination reaction. The CO_2/H_2O gas mixture could be separated by steam condensers,[19] whereas the CO_2/He mixture is separable by selective membranes.[20]

In the last years, the CaL process has acquired a great relevance as a 2nd generation technology for capturing CO_2 emissions from fossil fuel power plants.[21-22] In this process, the capture of CO_2 from flue gases is performed by means of the carbonation reaction of CaO (eq.1). The gas-solid reaction takes place in a high temperature fluidized bed reactor (around 650ºC) where the post-combustion flue gas containing a CO_2 concentration near 15% vol. is used to fluidize a bed of CaO solids at atmospheric pressure. The partially carbonated CaO particles are then transported into a second reactor (calciner) where CaO is regenerated by calcination at high CO_2 partial pressure and high temperatures (~950ºC). CaO particles regenerated from calcination are carried again to the carbonator to be used in a new cycle. It must be remarked that calcination under high CO_2 vol concentration is a must in the CaL process for CO_2 capture in order to avoid its dilution before extracting it from the calciner for compression and storage afterwards. On the other hand, carbonation for CO_2 capture is carried out at relatively low CO_2 vol concentration. Under these harsh conditions the multicycle conversion of natural limestone derived CaO suffers a drastic drop in just a few cycles. Numerous studies have been carried out on the use of additives or other techniques such as thermal pretreatment to mitigate the decay of the multicycle CaO activity, which is mainly caused by CaO grain sintering in the calcination stage.[23-24] Thus, the CaO multicycle conversion in short residence times at CaL conditions for CO_2 capture could be stabilized by the addition of nanostructured SiO_2[25-26] and thermal pretreatment,[27] which mitigate CaO sintering.

In the present work, natural limestone samples have been thermally pretreated by calcination under different atmospheres and the effect of thermal pretreatment on

their multicycle performance at CaL conditions for CSP energy storage has been studied for the first time to our knowledge. The effect of the addition of nanosilica on the multicycle CaO conversion at these conditions has been also newly tested. Although these techniques have been already employed in previous works[25-27] to observe their effect on the multicycle CaO conversion at CaL conditions for CO_2 capture, it must be remarked that CaL conditions for CSP energy storage differ radically from those used to capture CO_2, which may have an important effect yet unexplored on the role of the used techniques to enhance the multicycle CaO activity.

2. Materials and methods

High purity natural limestone (> 99% $CaCO_3$) from Matallagar quarry (Pedrera, Seville, Spain) has been used in our work as CaO precursor. Samples from different batches received (labeled as A and B) were employed with diverse concentration of impurities as seen from X-Ray fluorescence (XRF) measurements (Table 1) conducted using an Axios (PANalytical) spectrometer. Even though both samples exhibit a very high Ca content, the sample from batch A shows a larger amount of impurities. It is remarkable the relatively higher concentration of Mg in sample A, whose presence can be attributed to dolomite usually found as impurity in natural limestone. As reported in previous studies,[28] the multicycle CaL activity of CaO derived from dolomite is improved as compared to CaO derived from limestone. However, the presence of dolomite by a small amount in Limestone A is not expected to yield a significant improvement of performance.

Table 1. Elemental composition of natural limestone samples A and B from different batches used in our work as measured by XRF.

Elements	Ca	Mg	Al	Si	Fe	Na	K	P	S	Sr	Mn
Limestone A (wt%)	39,53	0,15	0,02	0,14	0,07	0,02	0,02	0,02	0,02	0,01	0,02
Limestone B (wt%)	40,04	0,09	-	0,02	0,01	-	-	0,01	0,02	0,01	-

In order to carry out the thermal treatments, a setup was built to calcine the samples under different gases, including super-heated steam, in a controlled way. Thus, besides of superheated-steam (SHS), thermal pretreatments were carried out under N_2, He and CO_2 atmospheres. Precalcinations were accomplished in a tube furnace and the hot junction of a thermocouple was placed on the top of the sample to accurately control the temperature during the calcination process (Figure 2**)**. The temperature was continuously monitored while the thermal pretreatment took place. When calcination was carried out under SHS, water was driven across the furnace by a peristaltic pump at a controlled flow rate.

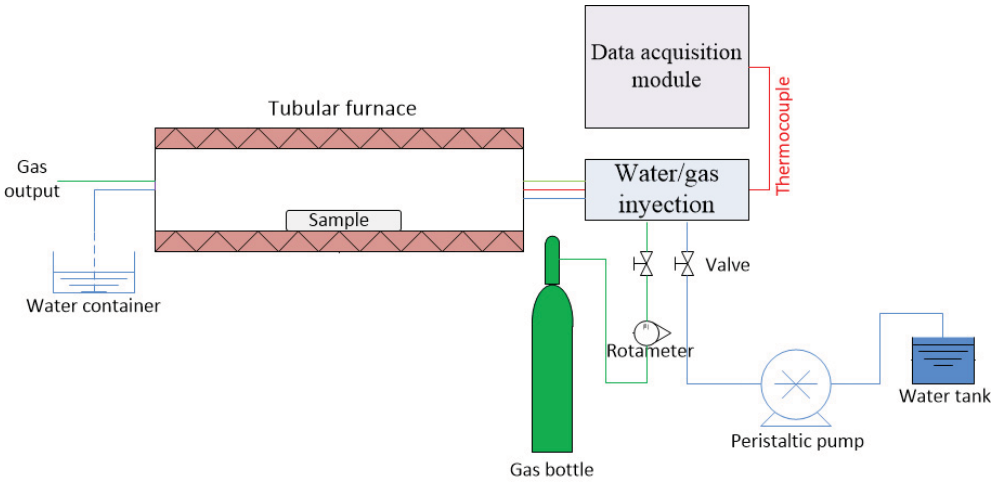

Fig.2. Thermal pretreatment furnace setup.

In each experiment, ~150 mg of the sample was weighed and placed in the middle of the furnace. Then, the gas/water injection system was connected and the sample heated to the minimum temperature required for attaining full decomposition under SHS or other gas selected. Thus, the samples were precalcined for 1 hour at 960ºC under CO_2, 760ºC under N_2 and 725ºC under He. Gas flow rates of 100 cm^3/min were employed in all cases. After calcination, the gas was switched to N_2 (100 cm^3/min) to avoid CaO hydroxylation and the temperature was decreased to room temperature.

When SHS was used for precalcination, the sample was preheated under a gas flow rate of 100 cm^3/min of N_2 up to ~600ºC and the temperature was kept constant for 30 min before introducing water into the chamber. This procedure was intended to minimize condensation inside the furnace since the goal was to carry out the thermal pretreatment under SHS. The water flow rate, controlled by the peristaltic pump, was 2 cm^3/min. Full

decomposition of the sample was obtained at 650ºC for 1 h under SHS. Then, a gas flow rate of N_2 of 100 cm^3/min was introduced in the chamber and the temperature decreased to room temperature.

Calcination/carbonation experiments were performed using a thermogravimetric analyzer (TGA) Q5000IR from TA Instruments. The instrument consists of a high sensitive balance (<0.1 mg) and a furnace heated by four IR halogen lamps that allow fast heating at controlled rates (300ºC/min) and stable isotherms. Each test consisted of 20 carbonation/calcination cycles at CaL conditions that maximize the efficiency of CSP storage, namely calcination at low temperature under He and carbonation under CO_2 at high concentration and high temperature with rapid transitions between the stages.[15] Quick switch between He for calcination and CO_2 for carbonation was achieved by using a gas flow rate of 200 cm^3/min. Each run was started with a precalcination stage at 725ºC during 5 min by quickly heating the sample from room temperature at a heating rate of 300ºC/min under a pure He gas flow of 200 cm^3/min. After precalcination the temperature was quickly increased (300ºC/min) to 850ºC and the gas switched to pure CO_2 with a gas flow of 200 cm^3/min for carbonation, which was maintained during 5 minutes. Once the carbonation stage was ended, the temperature was quickly decreased to 150ºC, the gas was switched to pure He and the temperature maintained for 2 minutes. Then, the sample was calcined again by increasing the temperature (300ºC/min) to 725ºC maintaining the He atmosphere. The temperature was then decreased again at 300ºC/min to 150ºC and maintained for 2 minutes under He, after which a new carbonation stage was started. The intermediate steps at 150ºC were introduced in order to mimic the extraction of sensible heat from the solids exiting the carbonator and calciner before storage, as proposed in the CaL-CSP integration scheme,[15] leading to a rapid cooling of the solids. The sample is placed inside a SiC enclosure heated by the IR halogen lamps, which minimizes undesired heat transfer phenomena. Samples of small and fixed mass (10 mg) were used to ensure an optimum heat and mass transfer during the gas- solid reactions occurring throughout the experiments.[29] TGA results reproducibility was checked in our work by performing runs at same conditions on different samples.

The samples were analyzed by X-ray diffraction (XRD) by means of a Miniflex 600 Rigaku operating at 40kV and 15mA and using radiation CuKα. Particle size distribution (PSD) was measured using a Mastersizer 3000. To this end, the samples

were dispersed in isopropanol and sonicated for a few seconds to facilitate particles dispersion. Specific surface and pore size distribution were studied by means of N_2 physisorption (ASAP2010 from Micromeritics). The microstructure of the samples was analyzed by scanning electron microscopy (SEM) employing a HITACHI S5200 SEM microscope.

3. Results and discussion

Thermal pretreatments of limestone A samples were driven on diverse atmospheres and under different temperatures to achieve full calcination for 1 h in all the cases as specified in Table 2. Furthermore, dry nano-silica powder was physically mixed with a sample of limestone A (15% nanosilica / 85% limestone wt/wt) after which the mixture was calcined in SHS. Hydrophilic nano-silica provided by Evonik (Aerosil®300 de Evonik Industries) was used to this end. Remarkably, full calcination under SHS was achieved under a relatively low temperature (650ºC) in agreement with previous studies, which has been attributed to a catalytic effect of H_2O on decarbonation in previous works.[30] On the other hand, calcination under pure CO_2 required a very high temperature (960ºC) as observed also elsewhere.[31]

Table 2. Calcination atmosphere and temperatures employed for thermal pretreatment (SHS: Super-heated steam).

Gas	**SHS**	**SHS with nanosilica (15% wt)**	**He**	**N_2**	**CO_2**
T (ºC)	**650**	**650**	**725**	**760**	**960**

The thermally pretreated samples were analyzed by X-ray diffraction (Fig. 3). When calcination was carried out under SHS, $Ca(OH)_2$ Bragg reflection peaks were observed (Fig.3d-e) possibly caused by water condensation in the tubular furnace due to temperature gradients, which may lead to partial hydroxylation. As expected, the XRD diffractograms show qualitatively a higher degree of crystallinity (narrower reflection peaks were obtained) for the sample pretreated under CO_2 (Fig. 3a) at high temperature, which favors solid-state diffusion during calcination thus leading to an enlargement of the CaO crystallite size.[32]

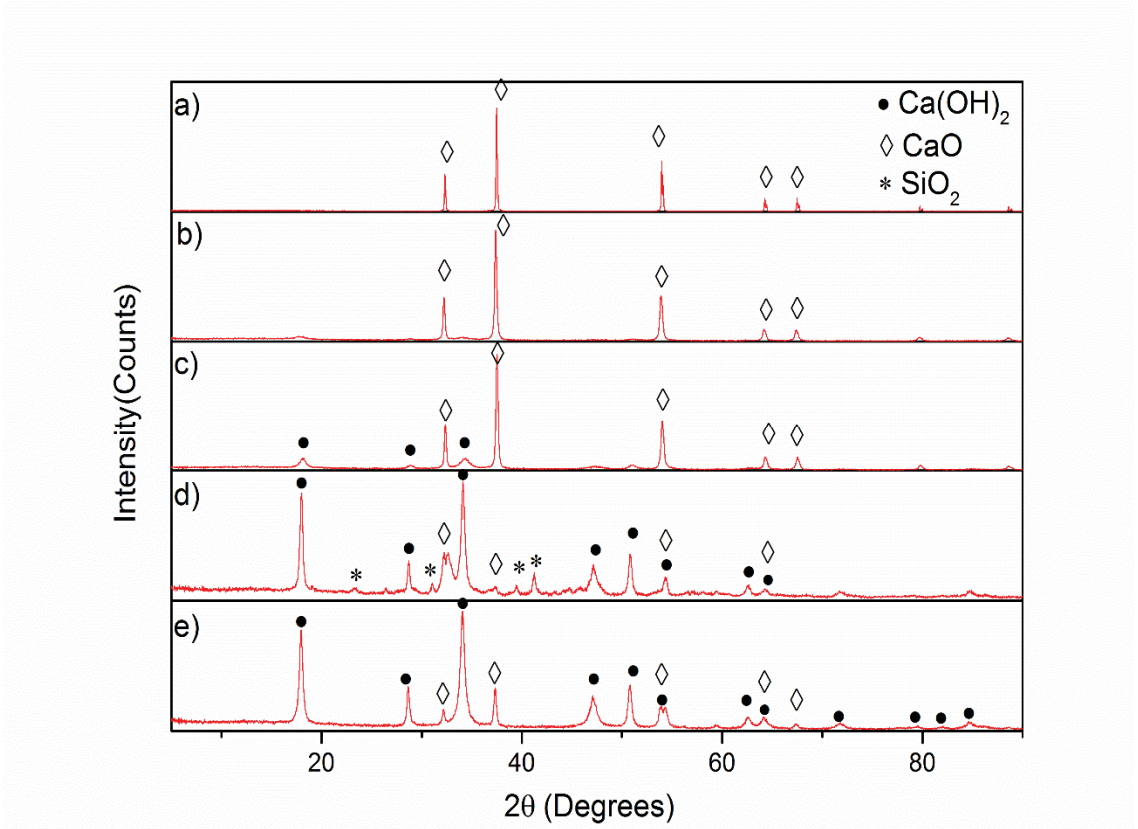

Fig. 3. X-Ray diffractograms of limestone A samples thermally pretreated for 1h under a) CO_2 at 960ºC, b) N_2 at 760ºC, c) He at 725ºC, d) SHS at 650ºC (mixed with nano-silica) and e) SHS at 650ºC.

To analyse the CaO multicycle activity behaviour under CaL-CSP conditions, CaO conversion in the Nth carbonation stage (X_N) was obtained from the thermograms (an example is shown in Fig.4) using equation (2), where W_{carb} is the mass of the sample at the end of the carbonation stage, W_{ini} is the mass of the sample just before carbonation and M_{CaO} and M_{CO2} are the molecular weights of CaO and CO_2 respectively.

$$X = \frac{(W_{carb} - W_{ini})}{W_{ini}} \frac{M_{CaO}}{M_{CO_2}} \qquad (2)$$

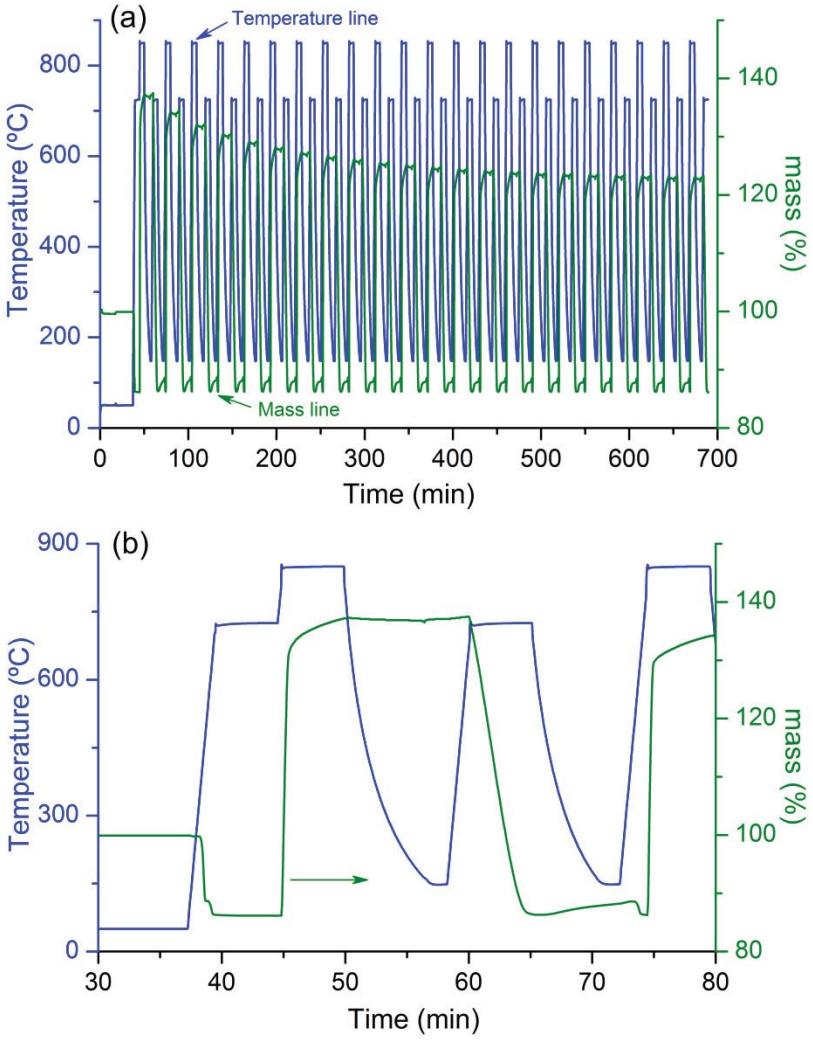

Fig. 4. (a) Time evolution of temperature and sample mass % along 20 carbonation/calcination cycles at CaL-CSP storage conditions for CaO resulting from limestone A pretreatment at 760ºC in N_2. The 1st cycle is detailed in (b). The slight drop in the weight baseline below 100% is due to partial carbonation and hydroxylation of the CaO sample that results from pretreatment which occurred between the end of the pretreatment and the start of the TGA test.

CaO multicycle conversion data are plotted in Fig.5 for all the pretreated samples over 20 carbonation/calcination cycles carried out under CaL-CSP storage conditions, and compared with the CaO multicycle conversion of the raw limestones A and B. For the sake of comparison, multicycle CaO conversion results obtained for

limestone A at CaL conditions for CO_2 capture reported elsewhere are also plotted in Fig. 5 (see ref. [22] for further details). As may be seen, the type of CaL conditions (either for CSP energy storage or CO_2 capture) determines fundamentally the multicycle performance of limestone derived CaO. Thus, the harsh calcinations employed at CaL conditions for CO_2 capture lead to a severe drop of CaO conversion after just a few cycles as widely reported in the recent literature.[22] On the other hand, CaO derived from raw limestone exhibits a relatively much higher multicycle activity at CaL conditions for CSP energy storage arguably due not just to the mild calcination conditions employed (relatively low temperature in absence of CO_2) but also because of the high temperature/high CO_2 concentration used for carbonation, which enhances significantly the carbonation reaction.

Let us now focus on the effect of pretreatment on the multicycle CaO conversion performance under CaL conditions for CSP energy storage. As seen in Fig. 5, thermal pretreatment under He, N_2 and SHS lead to similar performances as compared to the raw sample. On the other hand, the sample precalcined under CO_2 at high temperature presents initially a substantially lower activity presumably due to a drastic reduction of the CaO reactive surface area by enhanced sintering during pretreatment. Despite of the low initial activity caused by this pretreatment, a notable reactivation is observed along on the following cycles. Arguably, the low calcination temperature used in the cycles allows a progressive regeneration of CaO surface area resulting from decarbonation of the $CaCO_3$ formed after each cycle. The stable activity of the CaO resulting from the limestone pretreated under CO_2 at high temperature could be explained from the presence of macropores formed during thermal pretreatment that remain stable along the multiple CaL cycles. Macropore stability has been identified in the recent work by Xu et al.[33] as a key factor on improving the multicycle performance of CaO based sorbents in the CaL process. Previous works have also shown that the multicycle CaO stability is enhanced for thermally pretreated samples under high temperature.[34]

A relevant observation that can be made from Fig. 5 is that the limestone sample pretreated under SHS and mixed with nanosilica exhibits a rather low multicycle activity. As shown in Fig. 5 the initial CaO conversion for the nanosilica/CaO composite obtained in our work under CaL conditions for CSP energy storage is rather low and deactivation along successive cycles is not hindered. This poor performance contrasts with the observation reported in previous works on the use of nanosilica,[26]

which enhances the performance of the material at CaL conditions for CO_2 capture by mitigating the loss of CaO surface area due to sintering.

Regarding the multicycle behaviour exhibited by the different batches of raw limestone, Fig. 5 shows that sample B suffers a slightly more marked deactivation than sample A, which could be explained in principle by the concentration of impurities present in both samples having an effect on CaO sintering. However, the expected degree of CaO sintering is not significant at the mild CaL calcination conditions for CSP energy storage used in our tests and the concentration of impurities is quite small. As will be seen ahead, at these CaL conditions, the diverse mean particle size of the samples could play a relevant role through pore plugging.

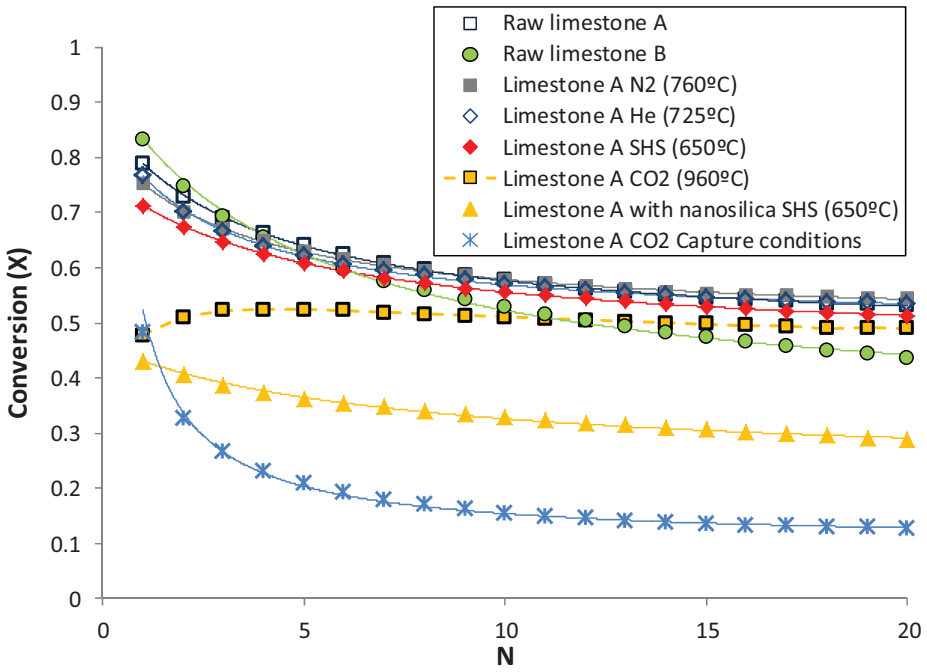

Fig. 5. CaO conversion of the sorbents derived from natural limestone (batches A and B) and pretreated samples of limestone A under different atmospheres (indicated in the inset) at CaL conditions for CSP energy storage. CaO conversion data obtained for limestone A cycled at CaL conditions for CO_2 capture are shown for comparison. [22] Solid lines are best fit curves of Eq. 3 to experimental data.

Multicycle CaO conversion data can be generally well fitted by the semi-empirical equation (3):[31, 35]

$$X_N = X_r + \frac{X_1}{k(N-1) + (1 - \frac{X_r}{X_1})^{-1}}; \quad (N = 1,2,..) \qquad (3)$$

Here X_1 is CaO conversion at the 1st cycle, N is the cycle number, k is the deactivation rate constant and X_r is the residual conversion towards which CaO conversion converges after a large number of cycles. Residual conversion values obtained from the best fits to conversion data are shown in Table 3, except for the sample pretreated under CO_2 whose behaviour does not conform to Eq. 3 and after 20 cycles shows a stable conversion close to 0.5. As seen in Fig. 5, Eq. 3, widely employed in the literature as fitting equation of multicycle CaO conversion data, provides a quite well fit to our experimental data ($R^2 > 0.99$), which allows us to reliably derive a value of the residual CaO conversion. Thus, the residual conversions derived for the limestone samples pretreated under different conditions (Table 3) are quite similar and close to 0.5 regardless of the gas and temperature used in these pretreatments. Thus, it may be concluded that thermal pretreatment determines the performance of the sample along the first cycles but the memory of this treatment is lost after a few cycles. On the other hand, an important effect is observed when nanosilica is added to the sample, which reduces considerably the residual conversion as opposed to the effect observed at CaL conditions for CO_2 capture.[25] Likewise, it is seen that the raw limestone samples from different batches show significantly different values of the residual conversions.

Table 3. Residual conversion of CaO from raw samples of limestone A and B and samples of limestone A pretreated under different atmospheres and temperatures and mixed with nanosilica.

Sample	**Limestone A**						**Limestone B**
	Raw	**SHS**	**SHS+nano-SiO_2**	**He**	**N_2**	**CO_2**	**Raw**
X_r	0.475	0.449	0.232	0.490	0.495	0.488	0.323

SEM analysis

All the thermally pretreated and raw samples were analysed by SEM in order to seek for a link between the surface morphology of the particles and multicycle CaO conversion data measured.

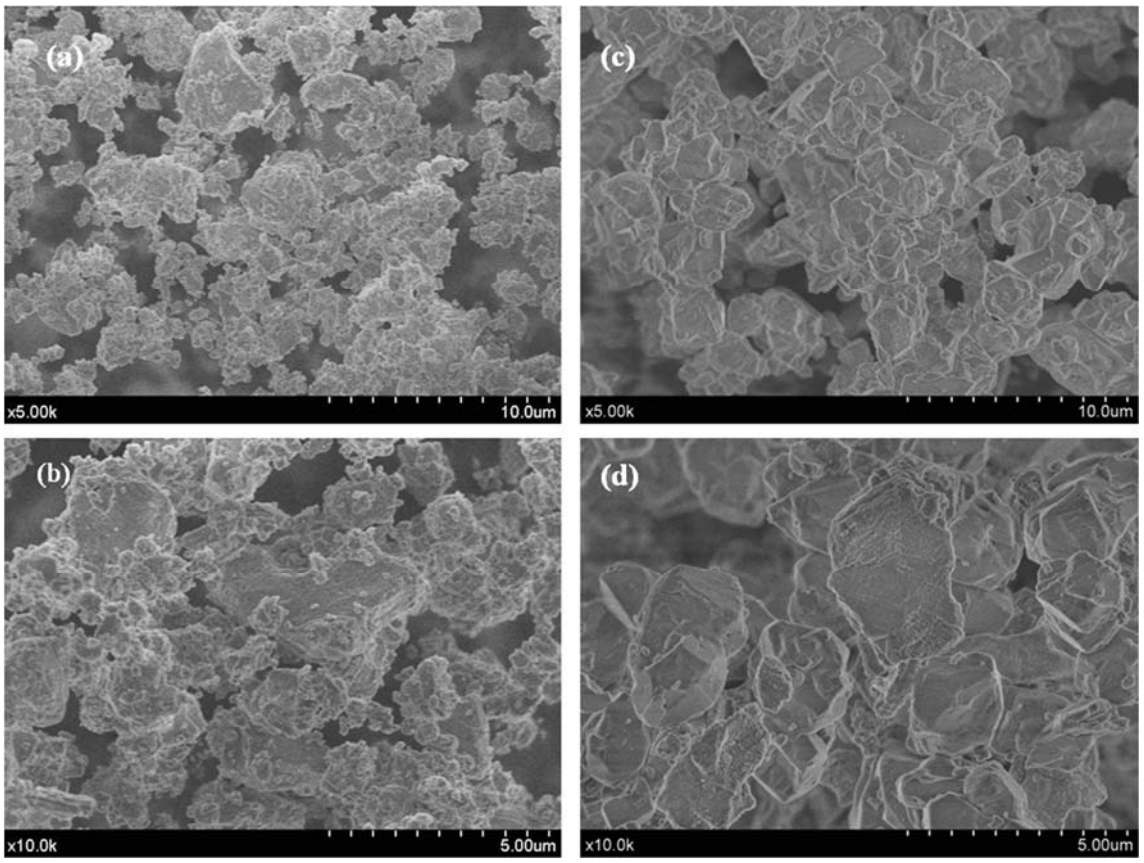

Fig. 6. SEM micrographs of raw samples of limestone A (a y b) and B (c y d).

Figure 6 shows micrographs of raw limestone samples A and B at different magnifications. As may be seen, the main difference inferred from these pictures is that sample A has a significant higher fraction of smaller micron-size particles as compared to sample B.

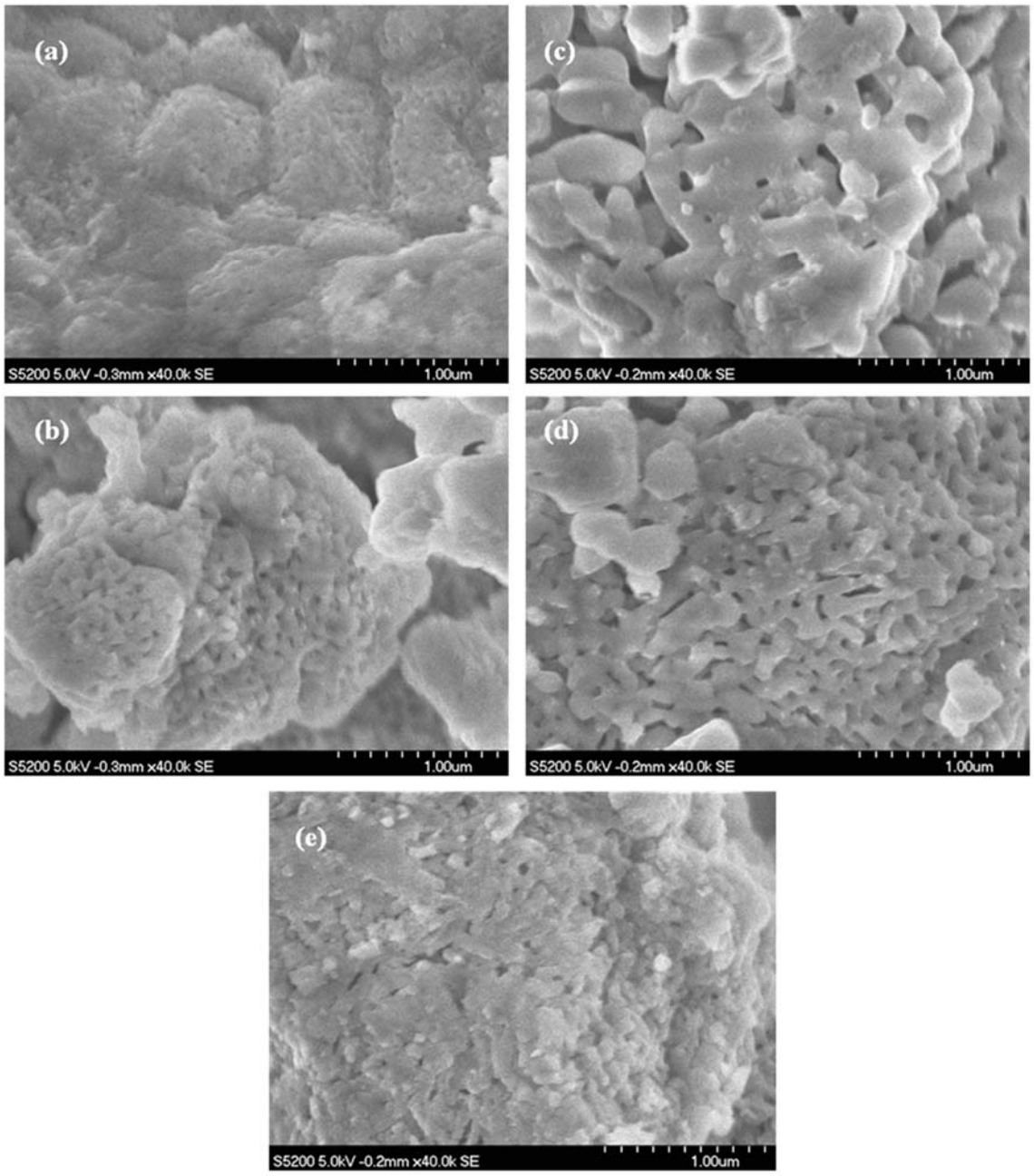

Fig. 7. SEM micrographs of limestone A pretreated samples in a) SHS (with nano-silica added), b) He, c) CO_2, d) N_2 and e) SHS.

SEM micrographs of pretreated limestone A samples are shown in Fig.7. These photographs give an idea on the porosity of the CaO skeleton that results from the thermal pretreatment. As can be seen, the different pretreatments carried out lead to significant differences in the CaO microstructure. Thus, the sample calcined under CO_2 at high temperature (Fig. 7c) presents a notably larger pore size and a marked sintering

of the CaO grains as would be expected from previous works.[36] On the opposite side, precalcination under SHS at relatively low temperature of the sample with added nanosilica yields significantly less sintering (Fig.7a) as could be anticipated from results reported in previous works showing a marked CaO sintering hindrance effect of nanosilica when used as additive.[25] In principle, this effect would lead to a large CaO surface area available for fast carbonation in apparent contrast with the detrimental effect of nanosilica addition on the multicycle CaO conversion obtained at CaL conditions for CSP energy storage (Fig. 5). This observation suggests that promoted sintering is not the main physical mechanism that determines CaO activity along carbonation/calcination cycles at CaL conditions for CSP storage.

Particle size distribution (PSD) analysis

Figure 8 illustrates the PSDs measured for the different samples analysed in our work after thermal pretreatment and before being subjected to the CaL cycles. Remarkably, the results suggest an inverse correlation between particle size and the residual CaO conversion of the samples. Fig. 9 shows data on the mean particle size obtained from the PSDs (D50) versus residual CaO conversion (X_r) values derived from the TGA tests. This correlation might be arguably caused by a physical phenomenon that would limit carbonation at the CaL conditions of our tests specific for CSP energy storage, namely pore plugging. At these conditions, carbonation at high temperature and high CO_2 pressure occurs very fast as seen in the thermogram shown in Fig. 4b. Moreover, the carbonate layer formed on the CaO surface during the fast reaction-controlled stage would reach a thickness over 100 nm at these high temperature and high CO_2 concentration.[37] On the other hand, calcination at the relatively low temperature for CaO regeneration would not lead to marked sintering thus yielding small pores (as will be seen below from the physisorption analysis). CaL conditions for CSP storage would thus favour the plugging of the small pores at the external surface of the particles, which would hamper the access of CO_2 to the interior of the CaO particles. As particle size is increased, pore plugging would thus impede carbonation on a relatively larger CaO surface area thus having a deeper negative impact on CaO conversion in the fast reaction controlled stage.

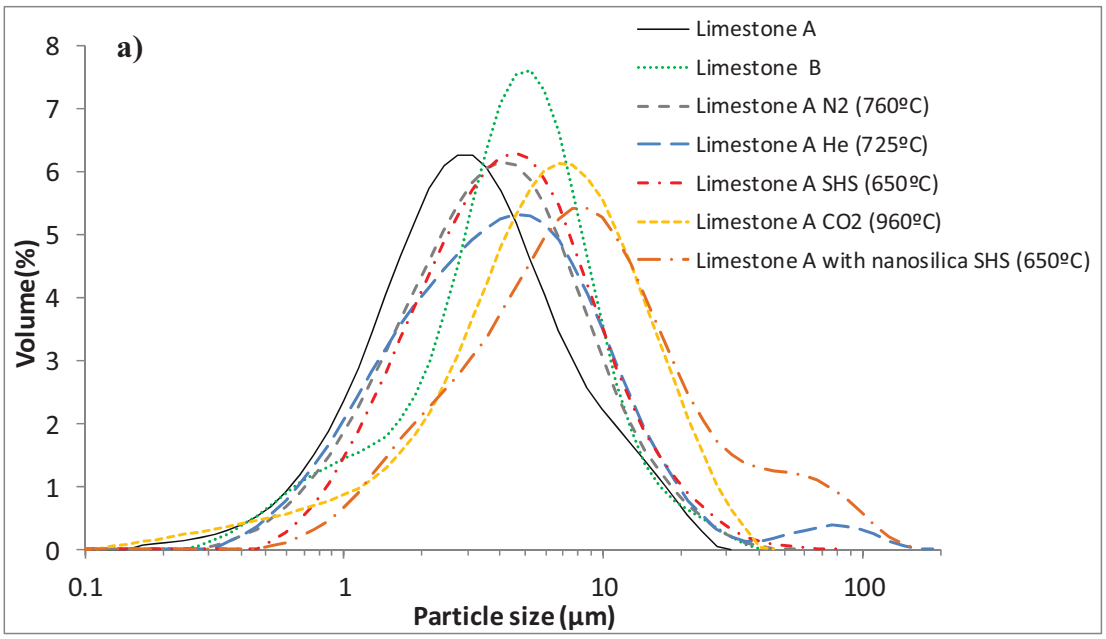

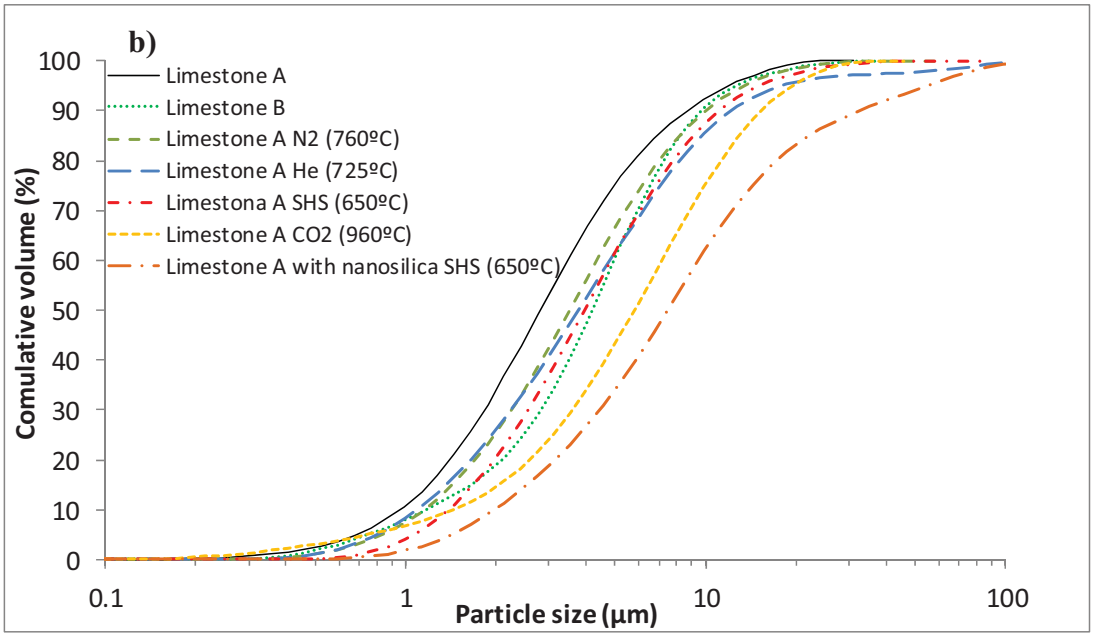

Fig. 8. a) Volume particle size distribution of CaO derived from raw and pretreated limestone A samples under different atmospheres and temperatures and from raw limestone B. b) Cumulative particle size distribution

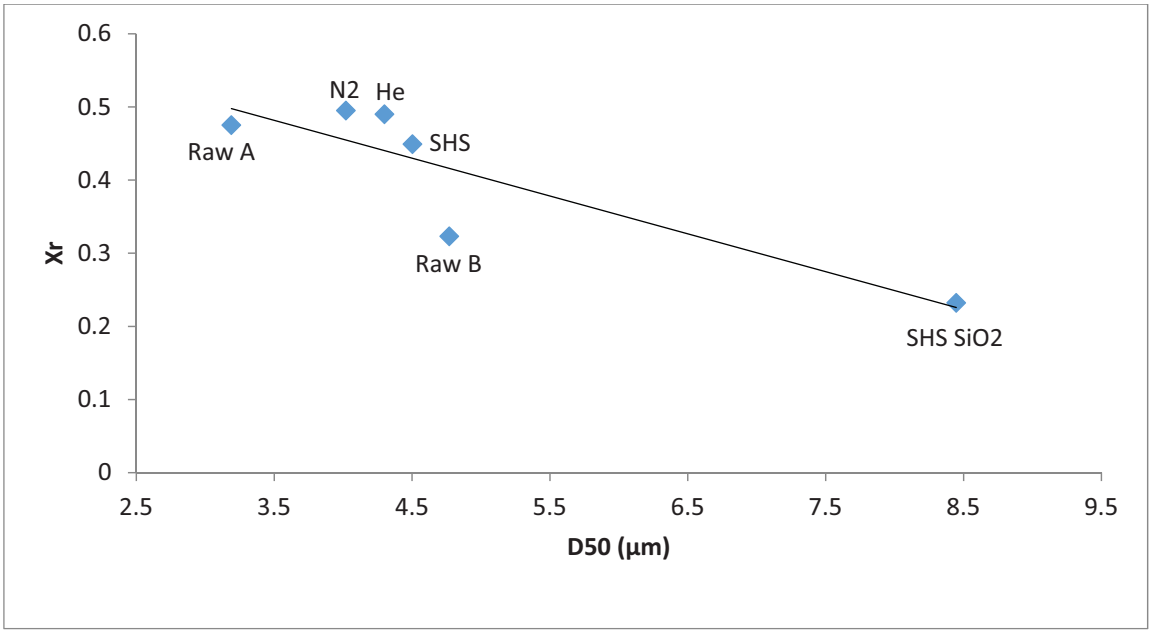

Fig. 9. Correlation between mean particle diameter (D50) and residual CaO conversion (Xr). The labels indicate the type of sample and for limestone A the gas under which thermal pretreatment was performed.

Physisorption analysis

Values obtained for the BET surface area of the pretreated samples are shown in Table 4. As would be expected, the addition of nanosilica leads to a significant increase of the surface area partly due to its nano-sized porous structure. Besides, nanosilica contributes to a reduction of CaO pore size in the mesoporous range as can be seen in the pore size distribution (Fig. 10).

Table 4. BET surface of limestone A samples pretreated under different atmospheres

Gas	SHS	SHS with nanosilica (15% wt)	He	N_2	CO_2	Limestone A (1st CSP cycle)
BET surface area (m^2/g)	**13**	**20**	**14**	**13**	**8**	**13**

Pore size distributions calculated by the BJH method are plotted in Fig.10. As can be seen, the thermally pretreated samples under N_2, He and SHS have a similar pore distribution with a main peak around 30-40 nm, which is consistent with the average size of the pores observed in the SEM micrographs (Fig.7). The similar particle size and pore size of these samples would explain why they show a similar multicycle CaO conversion behaviour as seen in Fig.5 if pore plugging were the driving factor that limits carbonation at the CaL conditions used. Even though the precalcination temperatures are diverse under these atmospheres, taking into account the small size of these pores and the carbonation conditions (high temperature and high CO_2 concentration), pore plugging would similarly limit carbonation for the CaO that stems from calcination under such diverse atmospheres. On the other hand, a noticeable effect of nanosilica is the shift of the mesoporous CaO pore size distribution to smaller pore sizes as was anticipated from our SEM analysis and previous works.[25] Since plugging of pores during carbonation becomes more likely as the size of the pores is decreased, CaO conversion would be further hampered as observed in our TGA tests (Fig 5). It must be also taken into account that the mean particle size of this sample is slightly larger than for the other samples (Fig.8), which would enhance further the detrimental effect of pore plugging.

The typical size of the carbonate layer that is quickly produced during the fast carbonation stage at CaL conditions for CSP energy storage (above 100 nm)[37] is larger than the mean pore size obtained from the pore size distributions, which reinforces the role of pore plugging on the multicycle CaO activity at these conditions. On the other hand, for the sample precalcined under CO_2, the SEM analysis (Fig. 7c) shows external pores of size over 100 nm. Although the size of macropores is out of range for N_2 physisorption analysis, previous analysis based on mercury intrusion porosimetry[38] have shown that calcination of limestone under CO_2 at high temperature (960ºC), which correspond to the same conditions of pretreatment in our test, shifts the CaO pore size distribution to sizes above 100 nm (peaking at 189 nm). In this case, there would be little surface area available at the first cycle for carbonation but pore plugging would not be relevant in limiting the reaction, which together with the stability of macropores generated by thermal pretreatment,[33-34] would allow for a stable multicycle CaO conversion as seen in Fig. 5.

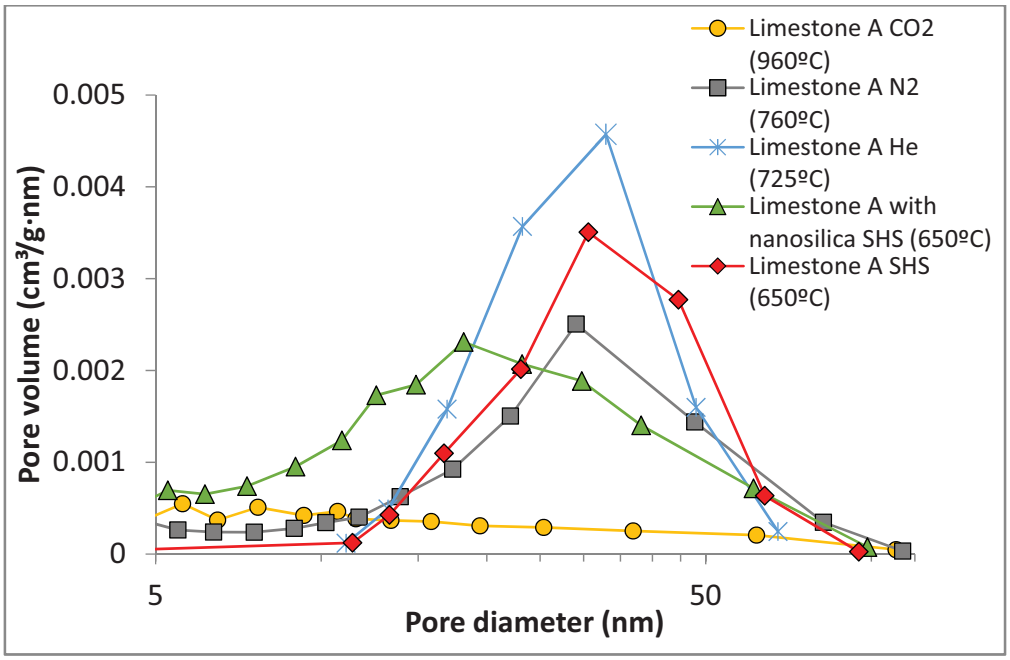

Fig. 10. Pore size distribution calculated by the BJH method for limestone A samples precalcined under different atmospheres as indicated.

The SEM picture in Fig. 11 shows the surface of a particle from the limestone A sample precalcined under N_2 and cycled at CaL conditions for CSP energy storage (ending in calcination) which further supports the argument on the important limitation posed by pore plugging on the CaO multicycle activity at these conditions. As may be seen, a part of the particle's surface has been broken during manipulation, which has left exposed a relatively porous CaO skeleton inside the particle whereas the rest of the surface is covered by a sintered CaO layer. Thus, only a relatively small fraction of the material at the particle's surface would be active along the carbonation/calcination cycles while the relatively porous CaO skeleton remains inaccessible to the CO_2. Pore plugging would be therefore a main limiting factor on carbonation in the fast reaction controlled regime, leading to a significant decay of the sorbent activity in short residence times with the number of cycles, which is further enhanced the larger the particle is.

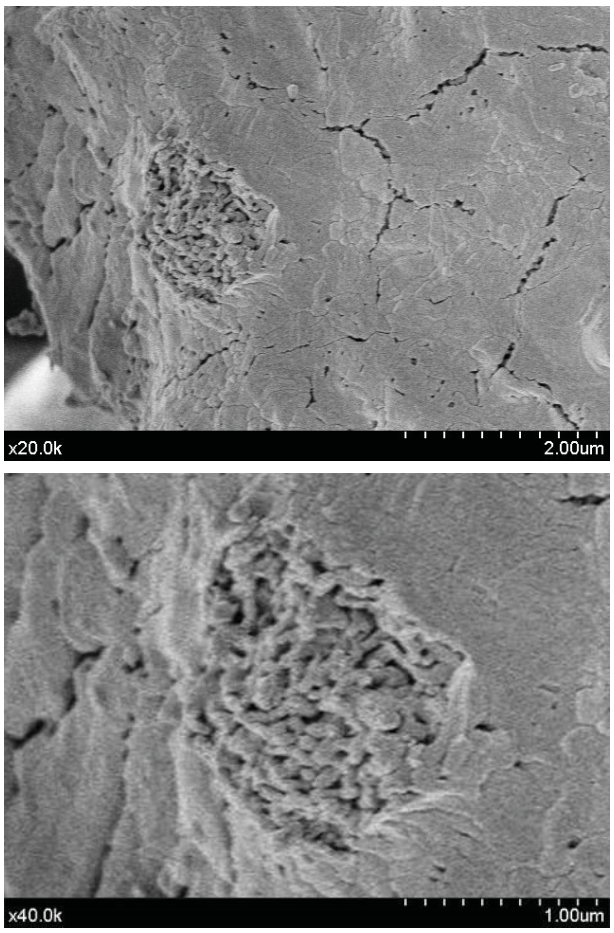

Fig. 11. SEM pictures of a limestone sample precalcined under N_2 after being subjected to CaL cycles at conditions for CSP energy storage (ending in calcination).

Further support to the argument on pore plugging as a main limiting factor on the multicycle CaO conversion performance of limestone at CSP-CaL conditions can be found in the experimental results reported by Lu et al.[39] who tested a number of CaO based sorbents at calcination conditions similar to those now judged as suitable for TCES in CSP plants involving a relatively low calcination temperature (700ºC) under He. Moreover, the CO2 vol% in Lu et al. tests was also relatively high in the carbonation stage, which was carried out in a window of temperatures extending up to 800ºC. As inferred from the results obtained, Lu et al. argued that a main factor limiting the CaO carbonation performance in multiple carbonation/decarbonation cycles was the plugging of pores rather than sorbent sintering in agreement with our observations. Additionally, Lu et al. observed that the addition of nanosilica did impair the sorbent carbonation performance at these carbonation/calcination conditions as we have also

seen in our work. It is also remarkable that the pore size distribution measured by Lu et al. after many cycles remained stable for a Ca-acetate based sorbent, which exhibited a stable conversion along the cycles.

The recent work by Pinheiro et al.[40] also points towards pore plugging as a determinant mechanism on the multicycle CaO carbonation performance when the CaO skeleton exhibits narrow bottleneck pore mouths susceptible of being blocked by the $CaCO_3$ product built upon the external surface of the particles. Thus, Pinheiro et al tested a number of CaO based sorbents and observed a poor performance for the samples with increased BET surface area and smaller pores, which is consistent with pore plugging as a relevant mechanism limiting carbonation in some cases. Interestingly, Pinheiro et al. observed this apparently anomalous behaviour by means of tests in a fixed bed reactor whereby calcination was carried out under N_2 at a relatively moderate temperature (800ºC), which would not cause excessive sintering of the regenerated CaO structure.

Experiments in fluidization environments should be pursued in future works to gain further knowledge on the sorbents' behaviour under CaL-CSP storage conditions. In particular, it would be interesting to investigate whether the significant improvement on powder flowability provided by the addition of nanosilica (as reported in ref. [41]), which increases the gas-solid contacting efficiency, would help improving the CaO carbonation performance in fluidized beds at CaL-CSP conditions thus counteracting its detrimental effect by enhancing pore plugging.

4. Conclusions

In this work we have analysed the role of thermal pretreatment and modification with nanosilica on the multicycle conversion performance of limestone derived CaO at Calcium Looping (CaL) conditions for Thermochemical Energy Storage (TCES) in Concentrated Solar Power plants (CSP). Limestone samples have been calcined under different atmospheres and the resulting CaO has been characterized by means of XRD, N_2 physisorption, SEM, and particle size analysis. The multicycle CaO activity of the precalcined samples under CaL conditions for CSP energy storage has been studied by means of thermogravimetric analysis (TGA). Importantly, CaL-CSP energy storage conditions radically differ from those used for CO_2 capture. The former involve carbonation at high temperature under high CO_2 partial pressure and calcination under relatively low temperature in the absence of CO_2 whereas the latter consist of

carbonation under low CO_2 partial pressure and calcination under high temperature and high CO_2 partial pressure. Thus, previous works have shown that the multicycle conversion of CaO derived from natural limestone at CaL conditions for CO_2 capture is mainly hindered by the drastic loss of CaO porosity and surface area available for fast carbonation due to enhanced sintering under harsh calcination conditions. On the other hand, our work shows that the multicycle CaO conversion at CaL-CSP energy storage conditions is rather limited by pore plugging, which is enhanced as CaO porosity and particle size are increased. Carbonation under high temperature and high CO_2 partial pressure leads to a very fast building up of a thick $CaCO_3$ layer in the fast reaction controlled stage. As a consequence, the small pore size caused by the mild calcination conditions favours pore plugging, which prevents CO_2 to reach a relatively high CaO surface area by pore diffusion at the interior of the particles. Thus, pore plugging would be a detrimental phenomenon in the application of the CaL process to CSP energy storage especially if relatively large particles should be employed in practice. In our work, this phenomenon has been observed to be critical for particles of size on the order of tens of microns. This can be an important issue to be assessed for the use in pilot-scale plants of circulating fluidized bed reactors, which usually require the use of particles of size on the order of hundreds of microns to avoid a significant loss of fine particles that cannot be recovered by conventional cyclones.

5. Acknowledgements

Financial support by the Spanish Government Agency Ministerio de Economia y Competitividad (contracts CTQ2014-52763-C2-2-R and CTQ2014-52763-C2-1-R) is acknowledged. The authors thank VPPI-US for the AP current contract and the RyC program for PESJ contract. The Microscopy, Functional Characterization and X-ray services of the Innovation, Technology and Research Center of the University of Seville (CITIUS) are gratefully acknowledged.

References

(1) Framework Convention on Climate Change. Adoption of the Paris Agreement. Proposal by the President. **2015**.

(2) Hinkley, J. T.; Hayward, J. A.; Curtin, B.; Wonhas, A.; Boyd, R.; Grima, C.; Tadros, A.; Hall, R.; Naicker, K. An analysis of the costs and opportunities for concentrating solar power in Australia. *Renew. Energy* **2013**, 57, 653-661.

(3) Reddy, V. S.; Kaushik, S. C.; Ranjan, K. R.; Tyagi, S. K. State-of-the-art of solar thermal power plants-A review. *Renew. Sust. Energ. Rev.* **2013**, 27, 258-273.

(4) Zhang, H. L.; Baeyens, J.; Degreve, J.; Caceres, G. Concentrated solar power plants: Review and design methodology. *Renew. Sust. Energ. Rev.* **2013**, 22, 466-481.

(5) Janz, G. J.; Allen, C. B.; Bansal, N. P.; Murphy, R. M.; Tomkins, R. P. T. Physical properties data compilations relevant to energy storage. II. Molten salts: data on single and multi-component salt systems. *(No. NSRDS-NBS-61 (Pt. 2)). Rensselaer Polytechnic Inst., Troy, NY (USA). Cogswell Lab.* **1979**.

(6) Bauer, T.; Breidenbach, N.; Pfleger, N.; Laing, D.; Eckand, M. Overview of molten salt storage systems and material development for solar thermal power plants. In Proceedings of the 2012 National Solar Conference for (SOLAR 2012), Denver, 2012.

(7) Parrado, C.; Marzo, A.; Fuentealba, E.; Fernandez, A. G. 2050 LCOE improvement using new molten salts for thermal energy storage in CSP plants. *Renew. Sust. Energ. Rev.* **2016**, 57, 505-514.

(8) Liu, M.; Tay, N. H. S.; Bell, S.; Belusko, M.; Jacob, R.; Will, G.; Saman, W.; Bruno, F. Review on concentrating solar power plants and new developments in high temperature thermal energy storage technologies. *Renew. Sust. Energ. Rev.* **2016**, 53, 1411-1432.

(9) Pfleger, N.; Bauer, T.; Martin, C.; Eck, M.; Worner, A. Thermal energy storage - overview and specific insight into nitrate salts for sensible and latent heat storage. *Beilstein J. Nanotechnol.* **2015**, 6, 1487-1497.

(10) Paksoy, H. Ö., *Thermal Energy Storage for Sustainable Energy Consumption: fundamentals, case studies and design*, Springer Science & Business Media, 2007.

(11) Mahlia, T. M. I.; Saktisandan, T. J.; Jannifar, A.; Hasan, M. H.; Matseelar, H. S. C. A review of available methods and development on energy storage; technology update. *Renew. Sust. Energ. Rev.* **2014**, 33, 532-545.

(12) Pardo, P.; Deydier, A.; Anxionnaz-Minvielle, Z.; Rouge, S.; Cabassud, M.; Cognet, P. A review on high temperature thermochemical heat energy storage. *Renew. Sust. Energ. Rev.* **2014**, 32, 591-610.

(13) Wentworth, W. E.; Chen, E. Simple thermal-decomposition reactions for storage of solar thermal-energy. *Sol. Energy* **1976**, 18, (3), 205-214.

(14) Sakellariou, K. G.; Karagiannakis, G.; Criado, Y. A.; Konstandopoulos, A. G. Calcium oxide based materials for thermochemical heat storage in concentrated solar power plants. *Sol. Energy* **2015**, 122, 215-230.

(15) Chacartegui, R.; Alovisio, A.; Ortiz, C.; Valverde, J. M.; Verda, V.; Becerra, J. A. Thermochemical energy storage of concentrated solar power by integration of the calcium looping process and a CO_2 power cycle. *Appl. Energy* **2016**, 173, 589-605.

(16) Ortiz, C.; Chacartegui, R.; Valverde, J. M.; Becerra, J. A. A new integration model of the calcium looping technology into coal fired power plants for CO_2 capture. *Appl. Energy* **2016**, 169, 408-420.

(17) Avila-Marin, A. L. Volumetric receivers in Solar Thermal Power Plants with Central Receiver System technology: A review. *Sol. Energy* **2011**, 85, (5), 891-910.

(18) Berger, E. E. Effect of steam on the decomposition of limestone. *Industrial and Engineering Chemistry* **1927**, 19, (1), 594-596.

(19) Sceats, M. G.; Horley, C. J. U.S. Patent Nº 8,807,993. Washington, DC: U.S. Patent and Trademark Office. **(2014)**.

(20) Taketomo, E.; Fujiura, M. U.S. Patent No. 4,482,360. Washington, DC: U.S. Patent and Trademark Office. **(1984)**.

(21) Blamey, J.; Anthony, E. J.; Wang, J.; Fennell, P. S. The calcium looping cycle for large-scale CO_2 capture. *Prog. Energy Combust. Sci.* **2010**, 36, (2), 260-279.

(22) Perejon, A.; Romeo, L. M.; Lara, Y.; Lisbona, P.; Martinez, A.; Valverde, J. M. The Calcium-Looping technology for CO_2 capture: On the important roles of energy integration and sorbent behavior. *Appl. Energy* **2016**, 162, 787-807.

(23) Valverde, J. M. Ca-based synthetic materials with enhanced CO_2 capture efficiency. *J. Mater. Chem. A* **2013**, 1, (3), 447-468.

(24) Florin, N. H.; Blamey, J.; Fennell, P. S. Synthetic CaO-Based Sorbent for CO_2 Capture from Large-Point Sources. *Energy Fuels* **2010**, 24, 4598-4604.

(25) Valverde, J. M.; Perejon, A.; Perez-Maqueda, L. A. Enhancement of Fast CO_2 Capture by a Nano-SiO_2/CaO Composite at Ca-Looping Conditions. *Environ. Sci. Technol.* **2012**, 46, (11), 6401-6408.

(26) Erans, M.; Manovic, V.; Anthony, E. J. Calcium looping sorbents for CO_2 capture. *Appl. Energy* **2016**, 180, 722-742.

(27) Valverde, J. M.; Sanchez-Jimenez, P. E.; Perez-Maqueda, L. A. High and stable CO_2 capture capacity of natural limestone at Ca-looping conditions by heat pretreatment and recarbonation synergy. *Fuel* **2014**, 123, 79-85.

(28) Sarrion, B.; Valverde, J. M.; Perejon, A.; Perez-Maqueda, L.; Sanchez-Jimenez, P. E. On the Multicycle Activity of Natural Limestone/Dolomite for Thermochemical Energy Storage of Concentrated Solar Power. *Energy Technol.* **2016**, 4, (8), 1013-1019.

(29) Koga, N.; Criado, J. M. The influence of mass transfer phenomena on the kinetic analysis for the thermal decomposition of calcium carbonate by constant rate thermal analysis (CRTA) under vacuum. *Int. J. Chem. Kinet.* **1998**, 30, (10), 737-744.

(30) Wang, Y.; Thomson, W. J. The effects of steam and carbon-dioxide on calcite decomposition using dynamic X-ray-diffraction. *Chem. Eng. Sci.* **1995**, 50, (9), 1373-1382.

(31) Valverde, J. M.; Sanchez-Jimenez, P. E.; Perejon, A.; Perez-Maqueda, L. A. CO_2 multicyclic capture of pretreated/doped CaO in the Ca-looping process. Theory and experiments. *Phys. Chem. Chem. Phys.* **2013**, 15, (28), 11775-11793.

(32) Valverde, J. M.; Sanchez-Jimenez, P. E.; Perez-Maqueda, L. A.; Quintanilla, M. A. S.; Perez-Vaquero, J. Role of crystal structure on CO_2 capture by limestone derived CaO subjected to carbonation/recarbonation/calcination cycles at Ca-looping conditions. *Appl. Energy* **2014**, 125, 264-275.

(33) Xu, Y. Q.; Luo, C.; Zheng, Y.; Ding, H. R.; Zhang, L. Q. Macropore-Stabilized Limestone Sorbents Prepared by the Simultaneous Hydration-Impregnation Method for High-Temperature CO_2 Capture. *Energy Fuels* **2016**, 30, (4), 3219-3226.

(34) Manovic, V.; Anthony, E. J. Thermal activation of CaO-based sorbent and self-reactivation during CO2 capture looping cycles. *Environ. Sci. Technol.* **2008**, 42, (11), 4170-4174.

(35) Grasa, G. S.; Abanades, J. C. CO_2 capture capacity of CaO in long series of carbonation/calcination cycles. *Ind. Eng. Chem. Res.* **2006**, 45, (26), 8846-8851.

(36) Valverde, J. M.; Sanchez-Jimenez, P. E.; Perez-Maqueda, L. A. Limestone Calcination Nearby Equilibrium: Kinetics, CaO Crystal Structure, Sintering and Reactivity. *J. Phys. Chem. C* **2015**, 119, (4), 1623-1641.

(37) Li, Z. S.; Fang, F.; Tang, X. Y.; Cai, N. S. Effect of Temperature on the Carbonation Reaction of CaO with CO_2. *Energy Fuels* **2012**, 26, (4), 2473-2482.

(38) Alvarez, D.; Abanades, J. C. Pore-size and shape effects on the recarbonation performance of calcium oxide submitted to repeated calcination/recarbonation cycles. *Energy Fuels* **2005**, 19, (1), 270-278.

(39) Lu, H.; Reddy, E. P.; Smirniotis, P. G. Calcium oxide based sorbents for capture of carbon dioxide at high temperatures. *Ind. Eng. Chem. Res.* **2006**, 45, (11), 3944-3949.

(40) Pinheiro, C. I. C.; Fernandes, A.; Freitas, C.; Santos, E. T.; Ribeiro, M. F. Waste Marble Powders as Promising Inexpensive Natural CaO-Based Sorbents for Post-Combustion CO_2 Capture. *Ind. Eng. Chem. Res.* **2016**, 55, (29), 7860-7872.

(41) Perez-Vaquero, J.; Valverde, J. M.; Quintanilla, M. A. S. Flow properties of CO_2 sorbent powders modified with nanosilica. *Powder Technol.* **2013**, 249, 443-455.